Observation of dynamic crossover and dynamic heterogeneity in hydration water confined in aged cement paste

2008 J. Phys.: Condens. Matter 20 502101

(http://iopscience.iop.org/0953-8984/20/50/502101)

IOP FTC
IOP PUBLISHING JOURNAL OF PHYSICS: CONDENSED MATTER
J. Phys.: Condens. Matter **20** (2008) 502101 (6pp) doi:10.1088/0953-8984/20/50/502101

FAST TRACK COMMUNICATION

Observation of dynamic crossover and dynamic heterogeneity in hydration water confined in aged cement paste

Y Zhang[1], M Lagi[1,2], F Ridi[2], E Fratini[2], P Baglioni[2], E Mamontov[3] and S H Chen[1,4]

[1] Department of Nuclear Science and Engineering, Massachusetts Institute of Technology, Cambridge, MA 02139, USA
[2] Department of Chemistry and CSGI, University of Florence, Sesto Fiorentino, Florence, I-50019, Italy
[3] Spallation Neutron Source, Oak Ridge National Laboratory, Oak Ridge, TN 37831, USA

E-mail: sowhsin@mit.edu

Received 24 September 2008, in final form 23 October 2008
Published 12 November 2008
Online at stacks.iop.org/JPhysCM/20/502101

Abstract
High resolution quasi-elastic neutron scattering is used to investigate the slow dynamics of hydration water confined in calcium silicate hydrate gel in an aged cement paste at supercooled temperatures. A super-Arrhenius to Arrhenius dynamic crossover of the average translational relaxation time $\langle\tau\rangle$ as a function of the inverse temperature is observed at $T_L = 231 \pm 5$ K, which coincides with a prominent peak in the differential scanning calorimetry cooling scan. The dynamic susceptibility $\chi_T(t)$ calculated using the experimentally determined temperature dependence of the self-intermediate scattering function shows direct evidence of the enhanced dynamic fluctuations and the associated growth in size of the dynamic heterogeneity in the confined water on approaching T_L.

(Some figures in this article are in colour only in the electronic version)

Ordinary Portland cement powder consists of calcium silicates, aluminates and alumino-ferrites. When it is combined with water, it forms a plastic paste that sets and eventually hardens to a rock-like consistency. During this curing process a series of chemical hydration reactions take place to form the corresponding hydrated phases, mainly calcium silicate hydrate (C–S–H), and to develop a 3D interconnected solid random network. Thus, water plays the central role during the overall hydration process, when cement gains the desired hardness and strength [1]. Understanding the dynamic behavior of water confined in the cement paste is therefore crucial for achieving complete control over its mechanical properties. On the other hand, the exotic phase behavior of the confined water is also a fascinating source of contemporary research on glassy liquids [2–5].

[4] Author to whom any correspondence should be addressed.

White cement, in contrast to ordinary Portland cement, lacks calcium alumino-ferrite phases. In this letter, we study the dynamics of water confined in white cement (water/dry cement = 0.4 by mass), and cured for eight days, with measurements made for four days subsequently using quasi-elastic neutron scattering (QENS).

We observed a dynamic crossover phenomenon at $T_L = 231 \pm 5$ K in water confined in a white cement paste. We also experimentally constructed the dynamic susceptibility $\chi_T(t)$ in the deeply supercooled temperature range. Thanks to the newly built state-of-the-art high resolution backscattering spectrometer BASIS at the SNS, we were able to extract the average translational relaxation time of glassy water at supercooled temperatures, as previously shown for calcium silicates and aluminates pure phases [6–8] at room temperature. This result completes our investigation conducted over the past few years on the dynamics of water confined in

different geometries: in 1D, MCM-41 [9], in 2D, a protein hydration layer [10] and, finally in 3D, cement paste (the present work). The dimensionality of the confinement turns out to play an important role in the characteristics of the slow dynamics, such as the power law exponent for the fractional Stokes–Einstein relation [11].

An example of the 3D confinement of water in cement paste can be pictured through the *Jennings colloidal model* (JCM) [12, 13]. As displayed in the inset of figure 1(a), C–S–H is composed of colloidal particles with radius of ∼1.5 nm that aggregate to form globules (small spheres in figure 1(a)). These globules cluster to form low density (LD) C–S–H regions within 24 h. The size of these pores inside the LD C–S–H is estimated to be around 1 nm [14–16], which corresponds to the interplanar space between the growing C–S–H lamellae [17, 18].

Because of the hydration process the LD C–S–H domains assemble to give a structure with larger pores connected by narrow channels called inter-LD regions. The sizes of these pores are reported to vary over a large range (approximately between 1 and 10 nm [14–16]). The LD C–S–H aggregates grow with time, and after one month all the water in the inter-LD C–S–H is consumed by the hydration reaction.

The JCM is consistent with the differential scanning calorimetry (DSC) thermogram recorded 11 days after the preparation (figure 1(a)). Two main features (peaks) are present, at 247 and 231 K, of which the second peak represents the main contribution. No peak is detected above 253 K, in the temperature range typical for the freezing of bulk water. Thus, at this hydration time all the unreacted water in the sample is strictly a kind of confined water in the solid matrix. According to the JCM, the two peaks visible in the cooling part of the thermograms are due to 'water reservoirs', i.e. relatively large pores interconnected through small channels, with nanometric diameter. In particular, the peak in the region between 253 and 238 K is due to water that is only accessible via the inter-LD pores [14, 19, 20]. The time evolution of this kind of water is strongly connected to the w/c ratio [14] and in our conditions is totally consumed after 28 days [22]. On the other hand, the peak at 231 K corresponds to pores inside the LD C–S–H domains.

Near infrared (NIR) experiments confirm that after eight days of setting the water in the cement paste is confined. Figure 1(b) reports the NIR spectrum registered at 123 K on a sample cured for 3 h. The absorption at 6070 cm^{-1} is considered as a fingerprint of hexagonal ice [21]. The absence of the 6070 cm^{-1} peak after eight days indicates that, at this hydration time, water is totally 3D confined in the LD C–S–H domains and cannot crystallize any longer. This is the kind of water that we observed in the neutron scattering experiment. A detailed description of the time evolution of both low temperature NIR and DSC experiments performed on the same cement/water paste can be found elsewhere [22].

The high resolution backscattering spectrometer BASIS at the spallation neutron source (SNS) in Oak Ridge National Laboratory (ORNL) is capable of measuring over a dynamic range as large as ±258 μeV with an elastic energy resolution of 3 μeV (FWHM), enabling studies of the diffusive dynamics

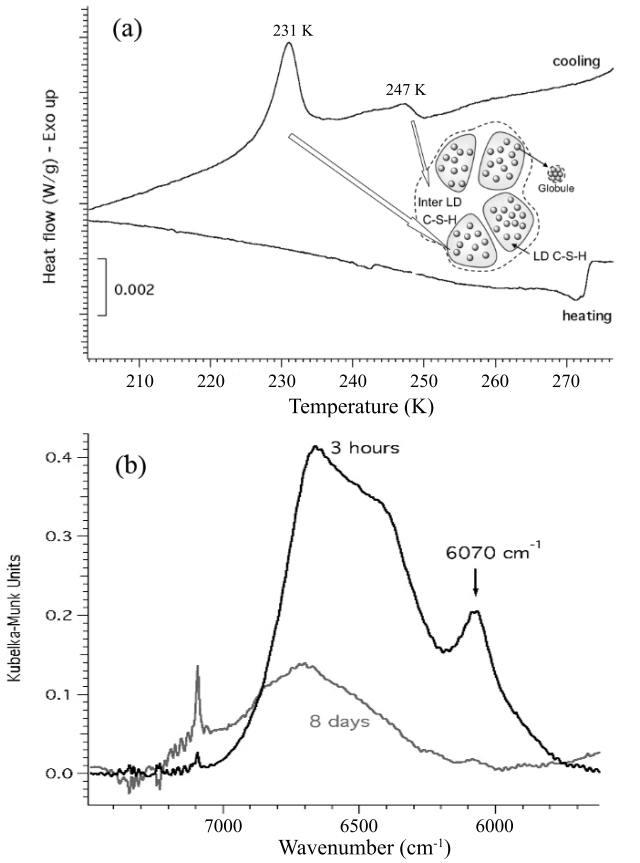

Figure 1. (a) DSC thermogram (cooling scan) of cement paste cured for 11 days. The inset displays a schematic representation of the Jennings colloidal model. According to the JCM, the peak at 247 K is due to inter-LD pore water and the peak at 231 K to LD pore water. (b) NIR spectra acquired at 123 K on cement paste cured for 3 h (black curve) and 8 days (gray curve).

of molecules on the atomic length scale. BASIS is an inverse geometry time-of-flight backscattering spectrometer that uses near backscattering neutron reflections from Si(111) analyzer crystals to select the final energy of the neutron of 2.08 meV (6.267 Å). The silicon analyzer crystals cover approximately 2.0 sr (16% of 4π). Neutrons are scattered by a sample illuminated by a polychromatic neutron beam, the bandwidth of which is defined by a set of neutron choppers. The dynamic range of the experiment can be adjusted by operating the choppers at either 60 Hz or a lower frequency. In this study, we operated the choppers at 30 Hz (matching the current accelerator frequency). For the data analysis, we selected a dynamic range from −100 to +100 μeV, which was free of excessive signal contamination that resulted from the instrument background, which was not yet fully optimized at the time of our experiment. When the experiment was carried out, the proton accelerator beam power on the mercury target was stabilized around 475 kW, which is only 1/3 of the designed power of 1.4 MW. Nevertheless, it is already the most intense pulsed neutron source in the world.

In this experiment, measurements were made on both an eight-days-old H_2O hydrated sample and a dry sample. The scattering from the dry sample was rather small due to the lack of hydrogen atoms, and thus was subtracted out

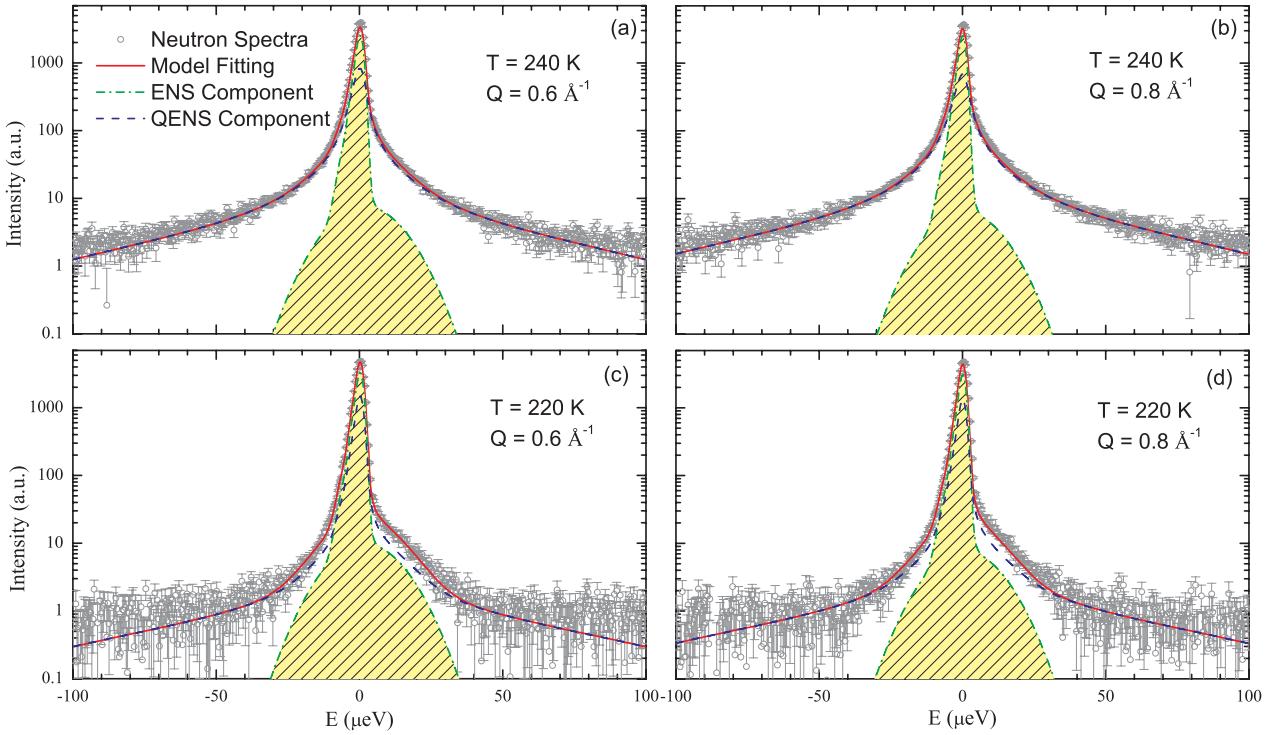

Figure 2. Illustration of the analysis of QENS spectra at two typical temperatures $T = 240$ K, 220 K and two typical wavevector transfers $Q = 0.6$ and 0.8 Å^{-1}, respectively. The hollow circles are the measured neutron intensity as a function of the energy transfer E. The solid line is the fitted curve using the model. The dash–dotted line area is the elastic scattering component, whose asymmetric shape derives from the asymmetric Q-dependent resolution function. The dashed line is the quasi-elastic scattering component.

as a background from the wet sample case. Due to the very large incoherent cross section of the hydrogen atom, neutrons are predominantly scattered by an incoherent process from the hydrogen containing species. The dynamics of the cement hydration water in the temperature range from 300 to 180 K, covering the dynamic crossover, varies from picosecond to nanosecond scale, so BASIS is the unique neutron scattering spectrometer for studying this phenomenon because of its capability of covering a wide dynamic range with high resolution.

QENS experiments essentially provide us with the incoherent dynamic structure factor $S_{\mathrm{H}}(Q, E)$ of hydrogen atoms in water molecules confined in the cement paste. The measured neutron spectrum is analyzed with the following relaxing cage model (RCM) [23], which has been tested extensively by means of MD simulations [23, 24] and QENS experiments [9, 10, 24–26]:

$$I(Q, E) = N\left[\begin{array}{l} f(Q)\delta(E)+ \\ (1-f(Q))FT\{F_{\mathrm{H}}(Q,t)\} \end{array}\right] \otimes R(Q, E) \tag{1}$$

where N is the normalization factor, $f(Q)$ is the elastic scattering component, taking into account the contribution coming from hydrogen atoms that cannot migrate over a dimension more than $2\pi/Q$ within the experimental observation time window. $F_{\mathrm{H}}(Q, t)$ is the self-intermediate scattering function (SISF), the Fourier transform of the incoherent dynamic structure factor $S_{\mathrm{H}}(Q, E)$, of the hydrogen atoms in the hydration water. $R(Q, E)$ is the Q-dependent energy resolution function as obtained by a low temperature run at 10 K with the hydrated sample, at which temperature all the relaxation processes are essentially frozen. A sum of Gaussian functions was used to represent the $R(Q, E)$ as follows:

$$R(Q, E) = \sum_i \frac{1}{\sqrt{2\pi}\sigma_i} \exp\left(-\frac{(E-E_i)^2}{2\sigma_i^2}\right). \tag{2}$$

It turns out that four Gaussian functions are sufficient for modeling the shape of the resolution function at each Q. They are then used to convolve with the expression contained between the brackets in equation (1) in order to fit the QENS spectra. Generally, the SISF is a product of the translational part, $F_{\mathrm{T}}(Q, t)$, and the rotational part, $F_{\mathrm{R}}(Q, t)$, i.e. $F_{\mathrm{H}}(Q, t) = F_{\mathrm{T}}(Q, t)F_{\mathrm{R}}(Q, t)$. By using only the spectra with $Q < 1$ Å^{-1}, the rotational contribution can be made negligibly small [23]. So the SISF is modeled as follows:

$$F_{\mathrm{H}}(Q, t) \approx F_{\mathrm{T}}(Q, t) = F^{\mathrm{S}}(Q, t) \exp\left(\frac{t}{\tau_{\mathrm{T}}(Q)}\right)^{\beta} \tag{3}$$

where the first factor, $F^{\mathrm{S}}(Q, t)$, represents the short-time vibrational motion of the water molecules in the cage. This factor affects the SISF on a sub-picosecond timescale, and thus is not an observable effect in this experiment. In the long-time limit (the timescale of α-relaxation process), $F^{\mathrm{S}}(Q, t)$ simplifies to its limiting value, the Debye–Waller

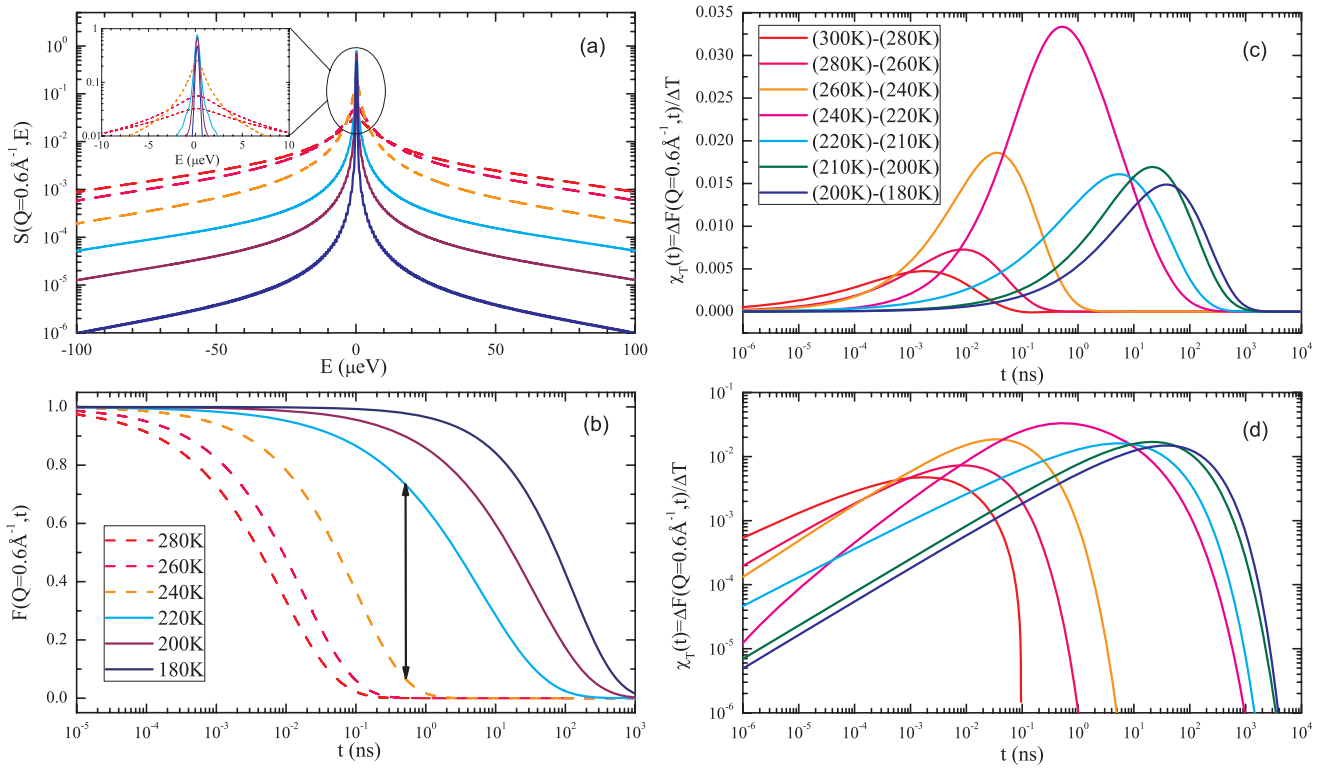

Figure 3. (a) Experimentally extracted incoherent dynamic structure factor $S_H(Q, E)$; the inset shows a zoom-in for the peak part. (b) Self-intermediate scattering function $F_H(Q, t)$. Three temperatures each are plotted above and below T_L. ((c), (d)) Dynamic susceptibility $\chi_T(t)$ on linear–log and log–log scales respectively. All the figures are plotted for $Q = 0.6$ Å^{-1}.

factor $F^S(Q, t) = \exp(-Q^2a^2/3)$, where $Q < 1$ Å^{-1} and $a = 0.5$ Å; thus it is approximately equal to $\exp(-1/12) \approx 1$ [23]. The second factor, the α-relaxation term, contains the stretch exponent β, and the Q-dependent translational relaxation time $\tau_T(Q)$, which is a strong function of temperature. $\tau_T(Q)$ follows a power law Q dependence as $\tau_T(Q) = \tau_0(aQ)^{-\gamma}$ where $a = 0.5$ Å [23]. The Q-independent average translational relaxation time, for the α-relaxation process, $\langle\tau\rangle$, is then evaluated as $\langle\tau\rangle = (\tau_0/\beta)\Gamma(1/\beta)$, where Γ is the Gamma function. It essentially gives a measure of the structural relaxation time of the hydrogen-bond cage surrounding a water molecule. The QENS spectra for each of the temperatures were analyzed for all four Q values (0.2, 0.4, 0.6 and 0.8 Å^{-1}) simultaneously to extract τ_0 and β, and consequently to evaluate the average α-relaxation time $\langle\tau\rangle$.

Examples of data analysis using the model discussed above are shown in figure 2. Two temperatures, one above T_L at 240 K and one below T_L at 220 K, are shown for two typical wavevector transfers $Q = 0.6$ and 0.8 Å^{-1}. The figures are plotted on a log scale to show the good agreement between the model and measured spectra over the whole intensity range. The elastic scattering component (shaded area), mainly from scattering of immobile water molecules, ranges from 58% at 300 K to 86% at 180 K, leaving enough scattering coming from the relaxation process of the hydrogen atoms in water molecules. Unlike for the dynamics at room temperature, the line shape of the quasi-elastic peak is non-Lorentzian ($\beta \approx 0.5$), indicating the glassy nature of the confined water.

The experimentally extracted incoherent dynamic structure factor, $S_H(Q, E)$, and its inverse Fourier transform, the SISF $F_H(Q, t)$, are shown in figures 3(a) and (b) for a representative $Q = 0.6$ Å^{-1}. The big gap between 240 and 220 K clearly visible in panel (b) is a consequence of the dynamic crossover in the translational relaxation time. Unlike for ideal glass forming liquids, the $F_H(Q, t)$ of this real physical system does not show an infinitely long plateau below T_c as predicted by the idealized mode coupling theory (MCT) [27]; instead, after struggling in the nanosecond time range, it decays to zero eventually through an α-relaxation process. The real structural arrest transition is avoided, which is likely due to the dynamic heterogeneity effect. To elucidate this point, the dynamic susceptibility $\chi_T(t) = \partial F_H(Q, t)/\partial T$, a measure of the temperature induced fluctuations, is calculated using finite differencing [28]. Experimentally, it is a much easier quantity to measure than the four-point dynamic susceptibility $\chi_4(t)$, which quantifies the amplitude of the spontaneous fluctuations; however, they are related to each other by the fluctuation-dissipation theorems [29]. Despite the fact that the temperature difference is 20 K (or 10 K), we can clearly see that $\chi_T(t)$ has a peak located at around $\tau(Q)$ in figure 3(c). The peak height is a measure of the volume within which the correlated motions take place. It grows on approaching T_L and reaches a maximum at T_L, but this growth is interrupted when the dynamic crossover sets in at T_L. This fact indicates that the dynamic fluctuations are enhanced near T_L, and lead to the maximum of the size of the dynamic

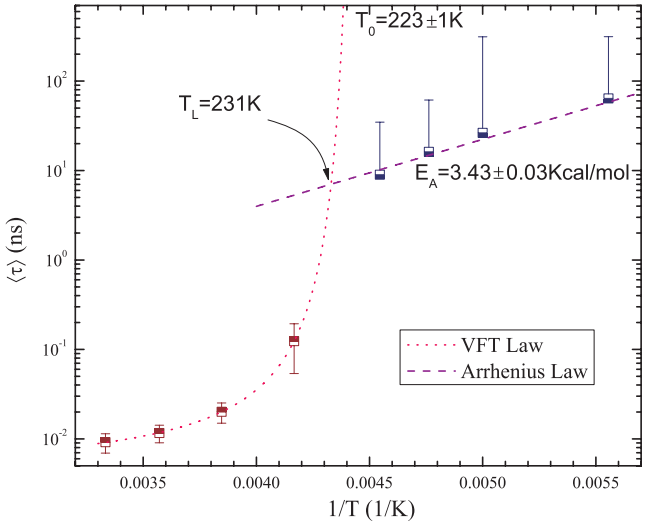

Figure 4. Arrhenius plot of experimentally extracted α-relaxation time versus $1/T$. An evidence of a super-Arrhenius (non-linear behavior) to Arrhenius (linear behavior) dynamic crossover is observed as the temperature is cooled through $T_L = 231 \pm 5$ K. The pink dotted and violet lines are the fittings of the VFT law and the Arrhenius law respectively. The error bars shown in the figure are calculated by error propagation. The real uncertainty could be less.

heterogeneity in the confined water being near T_L. Figure 3(d) plots the dynamic susceptibility on a log–log scale to show the power law dependence of $\chi_T(t)$ when $t < \tau(Q)$ as predicted by theory [29].

Figure 4 shows the Arrhenius plot of the experimentally extracted $\langle\tau\rangle$ versus $1/T$. It shows clear evidence of a super-Arrhenius (non-linear behavior) to Arrhenius (linear behavior) dynamic crossover as the temperature is cooled down through $T_L = 231 \pm 5$ K. The pink dotted and violet dashed lines are the fittings of the Vogel–Fulcher–Tammann (VFT) law $\langle\tau\rangle = \tau_{VFT} \exp[DT_0/(T - T_0)]$ and the Arrhenius law $\langle\tau\rangle = \tau_{Arr} \exp[E_A/(k_B T)]$ respectively with the same prefactor $\tau_{VFT} = \tau_{Arr}$. The resulting cusp-like behavior of the fitting functions allows us to extract the crossover temperature with accuracy, but the real dynamic transition could be smoother: the behavior of the two functions close to T_L is not meant to exactly reproduce the expected α-relaxation time values. The coincidence of the DSC peak and the dynamic crossover temperature at $T_L = 231 \pm 5$ K can also be understood with the Adam–Gibbs theory [30], where the slope of the Arrhenius plot of the mean α-relaxation time is directly related to the configurational entropy change.

The fragile-to-strong dynamic crossover at T_L could be interpreted as a variant of the kinetic glass transition temperature T_c predicted by the idealized MCT [27]. The structural arrest transition is avoided by activated hopping processes below T_L. The idealized MCT breaks down below T_L. Indeed, by treating hopping as arising from the vibrational fluctuations in a quasi-arrested state, an extended version of the MCT (eMCT) shows that the ergodic to nonergodic transition is replaced by a smooth crossover [31]. Furthermore, the dynamic theory eMCT also demonstrates the growing dynamic length scale when approaching T_L. The two predictions are experimentally verified in the present letter. Below T_L, any structural relaxation requires a cooperative rearrangement of a large cluster of water molecules connected through hydrogen bonds.

Our previous experiments [32] showed that the crossover temperature T_L marks the point below which the local structure of water is predominantly that of the LDL form. We may predict that below T_L, the structural properties of cement paste become drastically different from those above. Establishing to what extent this would affect the mechanical properties of the concrete at temperatures below T_L awaits future experiments.

Research at MIT is supported by DE-FG02-90ER45429; at the University of Florence by MIUR and CSGI. The neutron scattering experiment at Oak Ridge National Laboratory's Spallation Neutron Source was sponsored by the Scientific User Facilities Division, Office of Basic Energy Sciences, US Department of Energy. We benefited from affiliation with the European Union Marie Curie Research and Training Network on Arrested Matter. Ketton white cement was obtained as a generous gift by Castle Cement, through the Nanocem Consortium.

References

[1] Double D D and Hellawell A 1976 *Nature* **261** 486
[2] Debenedetti P G and Stanley H E 2003 *Phys. Today* **56** 40
[3] Mishima O and Stanley H E 1998 *Nature* **396** 329
[4] Debenedetti P G 2003 *J. Phys.: Condens. Matter* **15** R1669
[5] Angell C A 2004 *Annu. Rev. Phys. Chem.* **55** 559
[6] Fratini E, Chen S H, Baglioni P and Bellissent-Funel M C 2002 *J. Phys. Chem.* B **106** 158
[7] Fratini E, Chen S H and Baglioni P 2003 *J. Phys. Chem.* B **107** 10057
[8] Fratini E, Ridi F, Chen S H and Baglioni P 2006 *J. Phys.: Condens. Matter* **18** S2467
[9] Faraone A, Liu L, Mou C Y, Yen C W and Chen S H 2004 *J. Chem. Phys.* **121** 10843
[10] Chen S H, Liu L, Fratini E, Baglioni P, Faraone A and Mamontov E 1996 *Proc. Natl Acad. Sci.* **103** 9012
[11] Chen S H, Mallamace F, Mou C Y, Broccio M, Corsaro C, Faraone A and Liu L 2006 *Proc. Natl Acad. Sci.* **103** 12974
[12] Jennings H M 2000 *Cem. Concr. Res.* **30** 101
[13] Tennis P D and Jennings H M 2000 *Cem. Concr. Res.* **30** 855
[14] Snyder K A and Bentz D P 2004 *Cem. Concr. Res.* **34** 2045
[15] Jennings H M and Tennis P D 1994 *J. Am. Ceram. Soc.* **77** 3161
[16] Valckerborg R M E, Pel L and Kopinga K 2002 *J. Phys. D: Appl. Phys.* **35** 249
[17] Pratt P L and Jennings H M 1981 *Annu. Rev. Mater. Sci.* **11** 123
[18] Monteilhet L, Korb J P, Mitchell J and McDonald P J 2006 *Phys. Rev.* E **74** 061404
[19] Landry M R 2005 *Thermochim. Acta* **433** 27
[20] Thomas J and Jennings H M 2006 *Cem. Concr. Res.* **36** 30
[21] Grundy W M and Schmitt B 1998 *J. Geophys. Res.* **103** 25809
[22] Ridi F, Luciani P, Fratini E and Baglioni P 2008 *J. Phys. Chem.* B submitted
[23] Chen S H, Liao C, Sciortino F, Gallo P and Tartaglia P 1999 *Phys. Rev.* E **59** 6708
[24] Liu L, Faraone A, Mou C Y, Yen C W and Chen S H 2004 *J. Phys.: Condens. Matter* **16** S5403
[25] Liu L, Chen S H, Faraone A, Yen C W and Mou C Y 2005 *Phys. Rev. Lett.* **95** 117802

[26] Liu L, Chen S H, Faraone A, Yen C W, Mou C Y, Kolesnikov A I, Mamontov E and Leao J 2006 *J. Phys.: Condens. Matter* **18** S2261
[27] Gotze W and Sjogren L 1992 *Rep. Prog. Phys.* **55** 241
[28] Berthier L, Biroli G, Bouchaud J P, Cipelletti L, El Masri D, L'Hote D, Ladieu F and Pierno M 2005 *Science* **310** 1797
[29] Berthier L, Biroli G, Bouchaud J P, Kob W, Miyazaki K and Reichman D R 2007 *J. Chem. Phys.* **126** 184503
Berthier L, Biroli G, Bouchaud J P, Kob W, Miyazaki K and Reichman D R 2007 *J. Chem. Phys.* **126** 184504
[30] Adam G and Gibbs J H 1965 *J. Chem. Phys.* **43** 139
[31] Chong S H 2008 *Phys. Rev.* E **78** 041501
[32] Mallamace F, Broccio M, Corsaro C, Faraone A, Majolino D, Venuti V, Liu L, Mou C Y and Chen S H 2006 *Proc. Natl Acad. Sci.* **104** 424